MRE2019_3

by Leny Yuliati

Submission date: 20-May-2019 08:15AM (UTC+0700)
Submission ID: 1132996701
File name: 16._MRE2019_Response_surface_methodology.pdf (1.71M)
Word count: 6034
Character count: 28919

IOP Publishing Mater. Res. Express 6 (2019) 074004 https://doi.org/10.1088/2053-1591/ab180d

Materials Research Express

PAPER

RECEIVED
22 December 2018

REVISED
24 March 2019

ACCEPTED FOR PUBLICATION
10 April 2019

PUBLISHED
24 April 2019

Response surface methodology to optimize the performance of reduced graphene oxide-mesoporous carbon nitride photocatalysts

Leny Yuliati[1,2,3], Peggy Tiong[4] and Hendrik O Lintang[1,2,3]

[1] Ma Chung Research Center for Photosynthetic Pigments, Universitas Ma Chung, Villa Puncak Tidar N-01, Malang 65151, East Java, Indonesia
[2] Department of Chemistry, Faculty of Science and Technology, Universitas Ma Chung, Villa Puncak Tidar N-01, Malang 65151, East Java, Indonesia
[3] Centre for Sustainable Nanomaterials, Ibnu Sina Institute for Scientific and Industrial Research, Universiti Teknologi Malaysia, 81310 Johor Bahru, Johor, Malaysia
[4] Department of Chemistry, Faculty of Science, Universiti Teknologi Malaysia, 81310 Johor Bahru, Johor, Malaysia

E-mail: leny.yuliati@machung.ac.id

Keywords: reduced graphene oxide, mesoporous carbon nitride, RSM, light intensity, UV reduction duration, NPYR degradation

Abstract

The synthesis parameters to prepare the reduced graphene oxide-mesoporous carbon nitride photocatalyst by an *in situ* photocatalytic reduction of graphene oxide in the presence of mesoporous carbon nitride as the photocatalyst were investigated for degradation of *N*-Nitrosopyrrolidine (NPYR) under visible light irradiation. The optimum synthesis condition with optimized NPYR degradation was achieved on the composite sample with GO loading of 5 wt%, which was synthesized under low UV light intensity (0.4 mW cm^{-2}) and long UV reduction duration (24 h), while sonication time did not give a significant effect on the photocatalytic performance. From the response surface methodology (RSM) analysis, the predicted values were confirmed to be in good agreement with the experimental values with a high correlation coefficient (R^2) of 0.9989. This study also demonstrated that the predicted optimum NPYR degradation matched well with the experimental conditions. The radical scavenger tests revealed that the holes and superoxide radicals play as important active sites for photocatalytic degradation of NPYR on the rGO-*m*CN composite.

1. Introduction

The increase in the water and air pollution has been a great concern for the environmental remediation. In order to overcome this problem, photocatalysis technique has been proposed as one important approach to decompose the organic pollutants via an environmentally clean and safe process. Several metal oxides and composite photocatalysts have been developed and used for degradation of organic pollutants [1–3]. In this work, active composite photocatalysts consisting of reduced graphene oxide (rGO) and mesoporous carbon nitride (*m*CN) were synthesized and optimized for the degradation of nitrogen-containing pollutant, *N*-nitrosopyrrolidine (NPYR). The rGO was employed in the composite synthesis since it can act as a good electron shuttle or electron acceptor, where it is able to assist in electron transportation by capturing or accepting the photoexcited electrons from the semiconductor. Due to its superior electron conductivity, the rGO also can improve the electron conductivity of the semiconductor and contribute to better interfacial charge transfer on the rGO based semiconductor composites [4–8]. Various methods have been reported to reduce GO to rGO, such as chemical reduction, thermal reduction, and electrochemical reduction [9–14]. Of particular interest is the use of *in situ* photocatalytic reduction method to produce rGO based composites in the presence of a semiconductor photocatalyst and a sacrificial agent [15–18].

On the other hand, carbon nitride (CN) is a metal-free and non-toxic semiconductor with stacking graphitic and polymeric structure. Unfortunately, although the CN can act as a visible-light-driven photocatalyst, it still suffers from low photocatalytic performance due to less efficient in the separation of electron and hole. It has been proven that the two materials with similar layered geometric structure would form more effective

interfacial interaction [19–21]. Therefore, the CN that consists of the graphitic sheet-layered structure could provide an ideal surface to form good interactions with the rGO. These interactions would give rise to better interfacial charge transfer and charge separation as well as improved electron conductivity, owing to the presence of rGO as a good electron acceptor with superior electron mobility [15, 16, 19–21].

In order to investigate the important parameters to synthesize active reduced graphene oxide-mesoporous carbon nitride (rGO-*m*CN) composite by the *in situ* photocatalytic reduction method, detail studies were carried out by analyzing the effect UV light intensity, UV photocatalytic reduction duration, and sonication time on the activity towards the degradation of *N*-nitrosopyrrolidine (NPYR), which is a type of nitrosamine pollutant. In addition to the experiments, a computational study was also conducted by using a response surface methodology (RSM) software. The RSM has been reported as an analysis technique to evaluate the optimum reaction conditions as well as optimum synthesis condition with the use of minimum experimental runs [22–24]. Some studies also showed that the RSM gave a better accuracy compared to other modelling method such as Taguchi method [25, 26]. In the case of non-linear system, the Artificial Neural Network (ANN) has been shown to give a better accuracy as compared to RSM method [27–29]. However, this work demonstrated that the RSM was statistically significant and gave a very high correlation coefficient (R^2), which was 0.9989. Therefore, the RSM was proposed as a suitable modelling method to obtain the optimum synthesis methods of rGO-*m*CN for photocatalytic degradation of NPYR.

2. Experimental

2.1. Synthesis of GO, mCN, and rGO-mCN

The GO was synthesized according to the improved Hummers' method [30], while the *m*CN was synthesized by using cyanamide as the starting precursor to undergo thermal polymerization in the presence of 7 nm colloidal silica particles as the hard template to generate porosity [15]. Series of the rGO-*m*CN composites were produced in a similar approach to the previously reported photocatalytic reduction method using methanol as the sacrificial agent [15, 16]. As reported previously, 5 wt% GO was the optimum loading amount to give the highest activity for degradation of NPYR [15], and thus, the GO loading was fixed to 5 wt%.

In order to study the effect of UV light intensity, the rGO-*m*CN sample was synthesized under 24 h irradiation using 8 W UV lamp or 200 W UV lamp, which gave the light intensity of 0.4 mW cm^{-2} for 8 W lamp, 8 and 18 mW cm^{-2} for 200 W UV lamp. To study the effect of UV reduction duration, the rGO-*m*CN series were synthesized upon irradiation of 8 W lamp ($I = 0.4$ mW cm^{-2}) for 3, 6, 12, 24, and 30 h, or 200 W lamp ($I = 18$ mW cm^{-2}) for 3, 6, 12, and 24 h. Meanwhile, to investigate the effect of sonication time, the rGO-*m*CN composites were additionally sonicated for 0.5 h, 2 and 4 h before irradiated under 8 W UV lamp at a light intensity of 0.4 mW cm^{-2} for 24 h.

For comparison purpose, the rGO-*m*CN composite was also prepared by a chemical reduction method, in which NaBH4 was used as the strong reducing agent [9]. Another method, which was the thermal reduction method, was also used to synthesize the rGO-*m*CN similarly to the approach in the reported literature [10]. The rGO-*m*CN was also prepared by physically mixing GO and the *m*CN, by using a mortar and a pestle to produce a well-mixed sample.

2.2. Characterizations

The structural properties of GO, *m*CN, and rGO-*m*CN were investigated by x-ray diffractometer, Fourier-transform infrared (FTIR) and diffuse reflectance ultraviolet-visible (DR UV–vis) spectrophotometers, and scanning electron microscopy (SEM). XRD patterns were recorded on Bruker Advance D8 difframeter (Cu Kα radiation, $\lambda = 1.5406$ Å) with a scan rate of 0.05 ° s^{-1} in the range of 2θ of 5 to 60°. FTIR and DR UV–vis spectra were measured at room temperature on a Thermo Scientific Nicolet iS50 and Shimadzu UV-2600, respectively. For FTIR spectra measurements, potassium bromide (KBr) was used as a reference sample, in which the samples were mixed with KBr in the ratio of 1:9. For measurement of absorption spectra, barium sulfate ($BaSO_4$) was used as the reflectance standard material. The surface morphology of the samples was studied by SEM (JEOL JSM-6390LV microscope, accelerating voltage: 15 kV). Prior to the measurement, the sample was put on a carbon tape and coated with platinum.

2.3. Photocatalytic NPYR degradation

The photocatalytic NPYR degradation was carried out in a similar way to the reported one [15]. A solution of NPYR (50 ml, 100 ppm) and the photocatalyst (0.1 g) were added to a 100 ml round-bottom flask. Before reaction, the suspension was stirred for 4 h in a dark condition to ensure adsorption equilibrium. All the reactions were carried out in a closed system for 24 h under visible light irradiation (150 W, $\lambda > 400$ nm, $I = 500{,}000$ Lux). The solution was then filtered using a filter membrane (0.2 μm) and analyzed by a gas

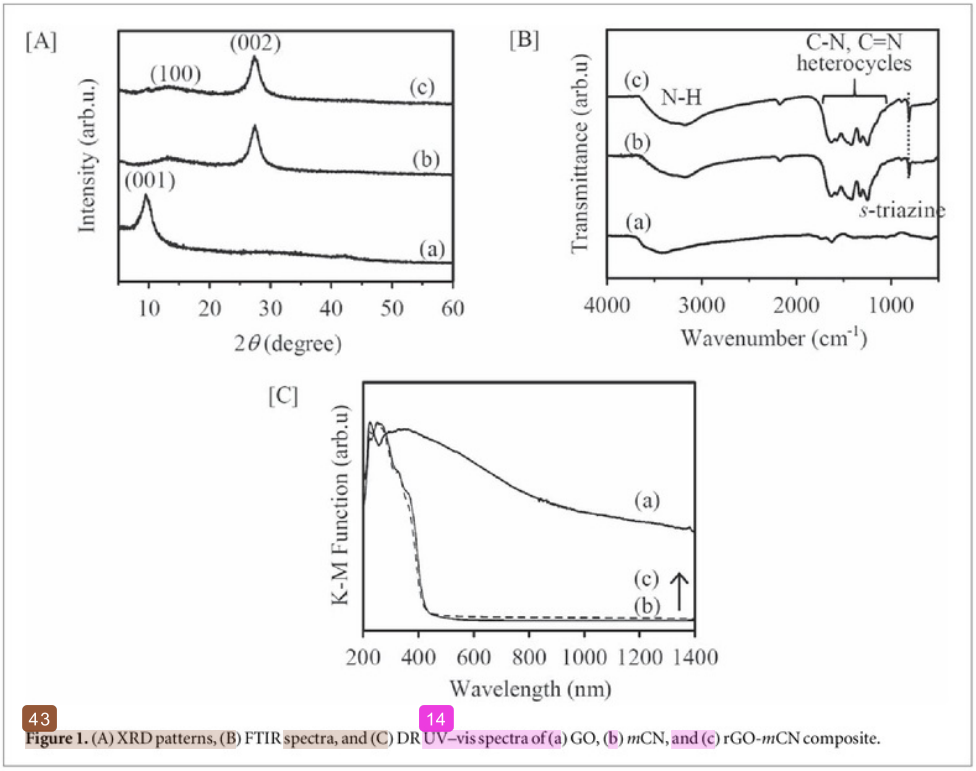

Figure 1. (A) XRD patterns, (B) FTIR spectra, and (C) DR UV–vis spectra of (a) GO, (b) *m*CN, and (c) rGO-*m*CN composite.

chromatography using a flame ionization detector (GC-FID) to determine the percentage degradation of the NPYR.

In order to determine the active species in NPYR degradation on the rGO-*m*CN, superoxide ($O_2^{\cdot-}$) radical and holes scavenger tests were conducted by using 1,4-benzoquinone (BQ) and di-ammonium oxalate monohydrate (AO), respectively. The mol ratio of added radical scavenger to the amount of NPYR was fixed to one. The radical scavenger was added into the mixture of photocatalyst and the NPYR solution 5 min before the light was turned on.

2.4. RSM analysis

The RSM based on a Box-Behnken design via Design-Expert software was used in order to examine the interactions among the investigated variables as well as to optimize the synthesis conditions of the rGO-*m*CN composite, where the photocatalytic performance for the NPYR degradation was set as the responding variable. Three independent variables in the synthesis of rGO-*m*CN composite via photocatalytic reduction method were selected: (i) light intensity of the UV lamp (mW cm^{-2}), (ii) UV reduction duration (h), and (iii) GO loading (wt%). These independent variables were assessed at three different levels, which were −1, 0 and +1, with different experimental values. For the effect of light intensity of the UV lamp, the light intensity employed was 0.4, 8, and 18 mW cm^{-2}. Meanwhile, the effect of UV reduction duration was evaluated at 6, 12, and 24 h. The effect of the different ratio of GO to *m*CN (wt%) was investigated at 1, 5, and 10 wt%. A total of 17 experiments was conducted with 5 replicates at the center point of the RSM analysis. This was done to ensure that an adequate prediction of results was comparable to the experiments in the evaluation of the selected quadratic model.

3. Results and discussion

The GO, *m*CN, and the prepared rGO-*m*CN composite were characterized by XRD, FTIR, DR UV–vis spectroscopies, and SEM. The characterization results are shown in figure 1. As has been also described elsewhere [15], the XRD patterns shown in figure 1(A) confirmed that the GO loading (5 wt%) did not affect the structural properties of the *m*CN. Displayed in figure 1(B) is the FTIR spectra of the samples, which also further confirmed that addition of GO did not affect the chemical structure of the *m*CN. On the other hand, a slightly

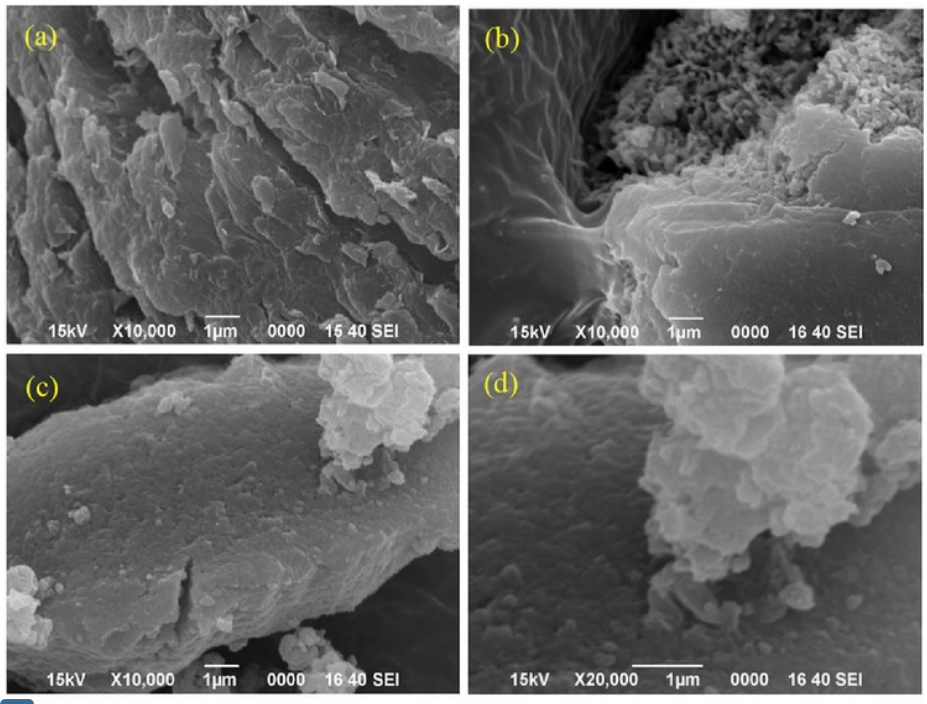

Figure 2. SEM images of (a) GO, (b) *m*CN, (c) and (d) rGO-*m*CN composite.

improved background absorption in the visible light region as compared to the *m*CN was observed on the rGO-*m*CN composite, as shown in figure 1(C).

SEM images of the rGO, *m*CN, and the rGO-*m*CN are shown in figure 2. From the SEM images depicted in figures 2(c) and (d), the rGO-*m*CN showed the characteristics of both the rGO and the *m*CN, but it was hard to differentiate the *m*CN from the rGO as both materials showed similar morphology stacking structure to each other.

As has been previously reported, the rGO-*m*CN showed photocatalytic activity for degradation of NPYR with percentage degradation of 34% [15]. In contrast, no activity was observed on the rGO-*m*CN was synthesized by thermal annealing. On the other hand, the rGO-*m*CN composites prepared via chemical reduction and physical mixing method exhibited 18 and 27% degradation, respectively. Among these investigated synthesis methods, the rGO-*m*CN composite prepared by the *in situ* photocatalytic reduction method gave the highest photocatalytic activity. This result clearly showed that the photocatalytic reduction method was the most feasible method under ambient conditions to synthesize the rGO-*m*CN composite photocatalyst for the degradation of NPYR.

Three UV light intensities (0.4, 8, and 18 mW cm^{-2}) were used in this study to investigate the effect of light intensity on the photocatalytic performance of the prepared composite samples. As can be seen in figure 3(A), the rGO-*m*CN prepared under UV light intensity of 0.4 mW cm^{-2} performed better in degradation of NPYR compared to the composite samples prepared under UV light intensity of either 8 or 18 mW cm^{-2}. About 34% of NPYR was successfully removed by the rGO-*m*CN prepared at low UV light intensity of 0.4 mW cm^{-2}, while only 18 and 16% of NPYR was removed by the rGO-*m*CN prepared at higher UV light intensity of 8 and 18 mW cm^{-2}, respectively. This result indicated that the light intensity of UV lamp in photocatalytic reduction method is crucial in optimizing the photocatalytic performance of rGO-*m*CN.

XRD measurement was performed on the rGO-*m*CN samples which were prepared at UV light intensities of 0.4 and 18 mW cm^{-2} as shown in figure 3(B). It was confirmed that the high UV light intensity did not impose great harm on the structural properties of the *m*CN. From the XRD patterns, all the rGO-*m*CN composite samples exhibited identical diffraction peaks to those of the *m*CN, even though different UV light intensities were used. This result suggested that the graphitic structure and the in-planar *s*-triazine arrangements of *m*CN and the rGO-*m*CN composite samples were similar to each other.

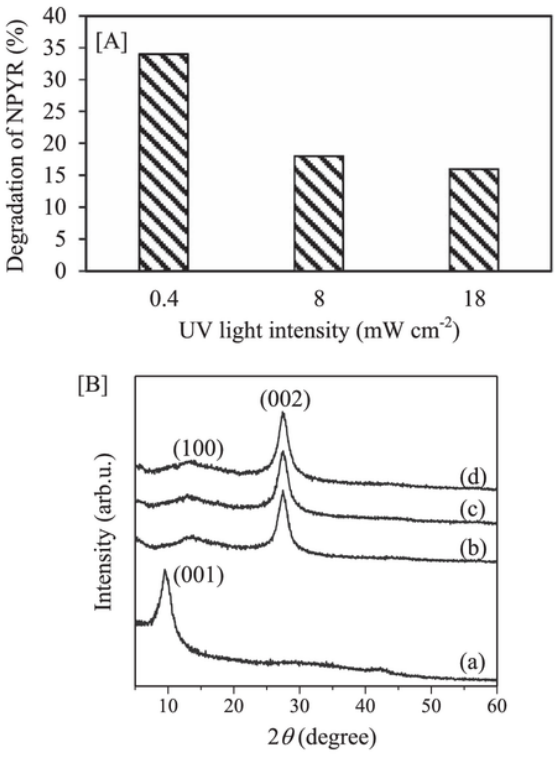

Figure 3. (A) Effect of UV light intensity on the photocatalytic performance of the rGO-*m*CN for the degradation of NPYR. The UV reduction duration was 24 h and sonication time was 0.5 h. (B) XRD patterns of (a) GO, (b) *m*CN, and rGO-*m*CN composites prepared under UV light with intensity of (c) 0.4 mW cm^{-2} and (d) 18 mW cm^{-2}. The UV reduction duration was 24 h and sonication time was 0.5 h.

Since the rGO-*m*CN prepared under UV light intensity of 8 and 18 mW cm^{-2} exhibited similar activity to each other, the effect of UV reduction duration (3–30 h) was investigated only on the rGO-*m*CN prepared under UV light intensity of 0.4 and 18 mW cm^{-2}. From figure 4(A), it was clear that the different UV light intensity gave the different optimum UV reduction duration. The optimum UV reduction duration for 0.4 and 18 mW cm^{-2} were 24 h and 6 h, respectively, which gave similar NPYR degradation of 34%.

For both UV light intensity, the photocatalytic performance was gradually enhanced when the duration of UV photocatalytic reduction increased at the early stage. This showed that the interrupted sp^2 network might be slowly restored by eliminating a large number of oxygen functional groups. For both UV light intensities, prolong the duration of photocatalytic reduction after the optimum point decreased the photocatalytic activity, which might be due to the presence of a large number of topological defects [11, 17].

In order to investigate the effect of UV reduction duration on the structural properties of the *m*CN, XRD measurement was performed on the rGO-*m*CN samples, which were prepared under 0.4 and 18 mW cm^{-2} of UV light intensity with different UV reduction times (3–30 h), as shown in figures 4(B) and (C). It was discovered that all the rGO-*m*CN composite samples exhibited identical diffraction peaks to those of the *m*CN, even though different UV reduction times were used.

It has been reported that to have good π-π stacking between aromatic structures of GO and *m*CN, the extent of exfoliation between layers of GO and *m*CN must be large enough so that both can interact well and produce a synergistic effect of rGO and *m*CN [4]. As the extent of exfoliation can be improved via sonication, the effect of sonication time during the synthesis process was investigated. In this study, three different sonication times, which were 0.5, 2 and 4 h, were employed to prepare the rGO-*m*CN samples under 24 h of 8 W UV irradiation with the intensity of 0.4 mW cm^{-2}. All the composite samples prepared by different sonication times showed the similar percentage of degradation, which was 34%, 32%, and 33%, respectively. This result suggested that 0.5 h was sufficient enough to exfoliate the layers of GO and *m*CN.

The structural properties of the composite samples were investigated and shown in figure 5. It can be observed that the sonication time did not disrupt the graphitic-layered structure and *s*-triazine arrangement of

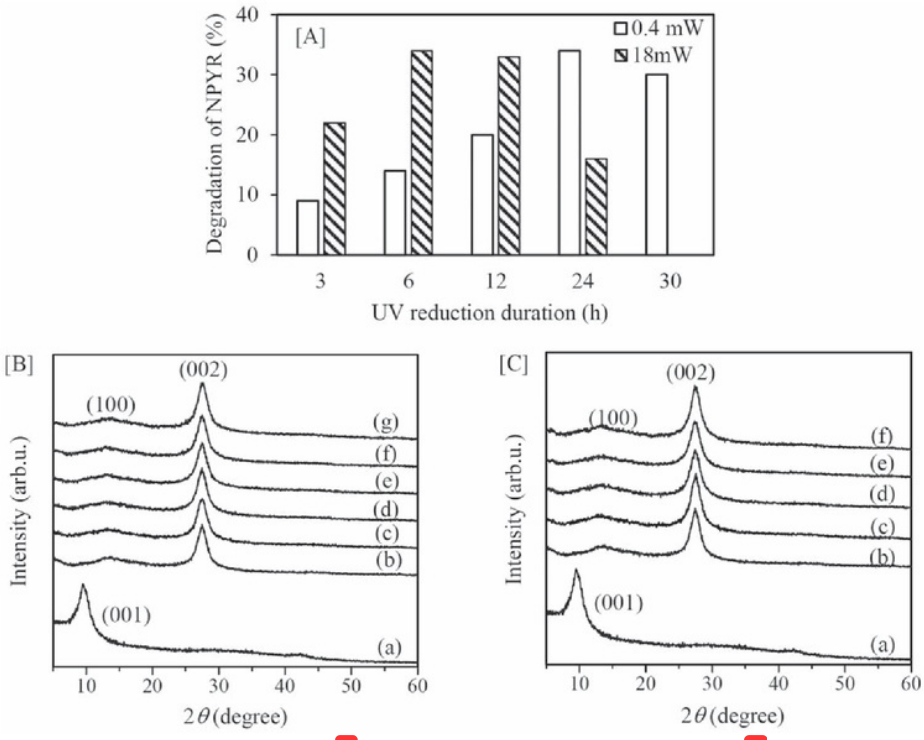

Figure 4. (A) Effect of UV reduction duration on the photocatalytic performance of the rGO-*m*CN prepared under UV light with an intensity of 0.4 or 18 mW cm^{-2} and sonication time of 0.5 h. (B) XRD patterns of (a) GO, (b) *m*CN, and rGO-*m*CN composites prepared under UV light (0.4 mW cm^{-2}) for (c) 3 h, (d) 6 h, (e) 12 h, (f) 24 h, and (g) 30 h. (C) XRD patterns of (a) GO, (b) *m*CN, and rGO-*m*CN composites prepared under UV light (18 mW cm^{-2}) for (c) 3 h, (d) 6 h, (e) 12 h, and (f) 24 h.

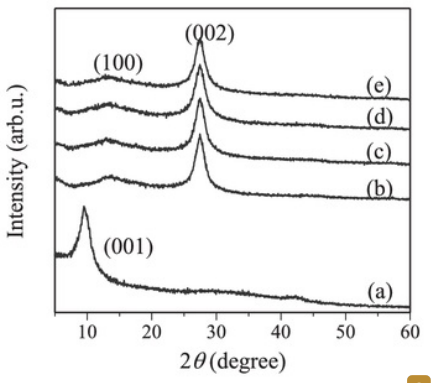

Figure 5. XRD patterns of (a) GO, (b) *m*CN, and rGO-*m*CN composites prepared by sonication for (c) 0.5 h, (d) 2 h, and (e) 4 h. All the rGO-*m*CN composites were synthesized under 24 h irradiation of UV lamp with a light intensity of 0.4 mW cm^{-2}.

the *m*CN. However, the rGO-*m*CN obtained under 4 h of sonication time showed a slight decrease in diffraction intensity as compared to the *m*CN. This might indicate that the prolonged sonication time would affect the ordered graphitic structure of the *m*CN but it did not give a significant effect on the photocatalytic performance of the composite sample.

In this study, the RSM based on a Box-Behnken design was selected in order to investigate the interactions of the investigated variables as well as to optimize the synthesis conditions on the responding variable. According to the experimental design in table 1, the mathematical relationship between the independent variables and the

Table 1. Experimental runs of the Box-Behnken design with the comparison between predicted and experimental NPYR degradation.

Standard	Run	Coded			Degradation (%)	
		A	B	C	Experiment	Predicted
9	1	0	−1	−1	17.13	17.23
8	2	1	0	1	18.13	18.37
2	3	1	−1	0	33.84	33.87
3	4	−1	1	0	34.54	34.52
16	5	0	0	0	15.99	16.22
11	6	0	−1	1	11.23	10.96
17	7	0	0	0	16.03	16.22
7	8	−1	0	1	21.18	21.31
6	9	1	0	−1	25.45	25.32
12	10	0	1	1	18.13	18.03
5	11	−1	0	−1	18.48	18.23
1	12	−1	−1	0	13.56	13.70
15	13	0	0	0	16.68	16.22
10	14	0	1	−1	15.35	15.62
13	15	0	0	0	16.35	16.22
14	16	0	0	0	16.07	16.22
4	17	1	1	0	18.64	18.50

Table 2. ANOVA results for a quadratic model of rGO-*m*CN synthesis using the Box-Behnken design.

Source	Sum of Squares	Degree of freedom	Mean square	F-value	p-value
Model	654.10	9	72.68	724.63	< 0.0001
A	8.61	1	8.61	85.86	< 0.0001
B	14.85	1	14.85	148.07	< 0.0001
C	7.49	1	7.49	74.66	< 0.0001
AB	327.25	1	327.25	3262.83	< 0.0001
AC	25.10	1	25.10	250.26	< 0.0001
BC	18.84	1	18.84	187.80	< 0.0001
A^2	214.38	1	214.38	2137.48	< 0.0001
B^2	13.42	1	13.42	133.84	< 0.0001
C^2	27.37	1	27.37	272.88	< 0.0001
Residual	0.70	7	0.10		
Lack of fit	0.36	3	0.12	1.42	0.3605
Pure error	0.34	4	0.085		
Total	654.80	16			

responding variable can be expressed by a second-order polynomial equation as shown in the equation (1) below.

$$\text{NPYR degradation (\%)} = 16.22 + 1.04A + 1.36B - 0.97C - 9.05AB - 2.51AC + 2.17BC + 7.14A^2 + 1.79B^2 - 2.55C^2 \quad (1)$$

where A, B, and C are the coded independent variables, corresponding to UV light intensity, UV reduction duration and GO loading, respectively. The predicted values were confirmed to be very close to the experimental values, suggesting a good agreement between the predicted and experimental values.

The experimental data were statistically analyzed by using an ANOVA and listed in table 2. According to the ANOVA results for quadratic response surface model, an R^2 of 0.9989 was obtained for the degradation of NPYR, suggesting that 99.89% of t variations could be explained by the independent variables within the investigated range and only 0.11% of the total variations could not be explained. Moreover, the hig alue of R^2 further suggested a good fitting between the model and the experimental data. It was reported that a good fit of a model should attain at least an R^2 value of 0.80 [31]. The obtained adj-R^2 of 0.9975 was very close to the R^2 value, indicating the presence of excellent correlations between the studied independent variables. On the other hand, the pred-R^2 shows the reliability of prediction of a model for new observations. The pred-R^2 and the adj-R^2 should be within 0.20 to each other. Otherwise, there might be outliers or model error present. The obtained pred-R^2 value was 0.9903, which was in reasonable agreement with the adj-R^2. Additionally, a low coefficient variation (C.V) of 1.65 also proved a good precision and reliability of the experiments.

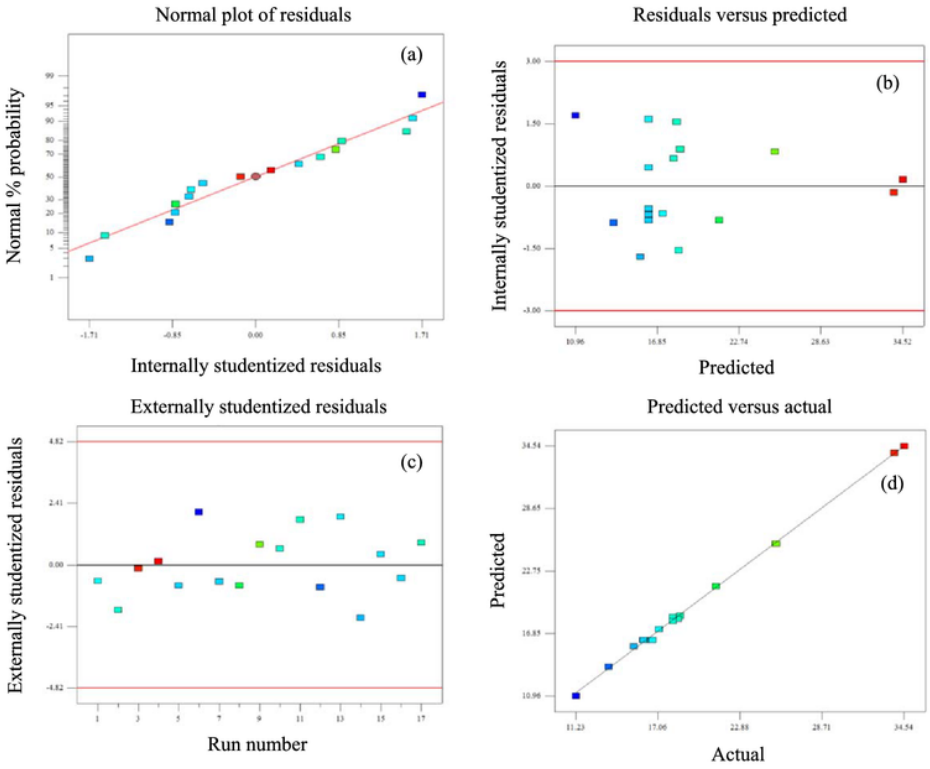

Figure 6. Diagnostic plots for evaluation of the adequacy, (a) normality, (b) internally studentized residuals, (c) externally studentized residuals, and (d) actual and predicted NPYR degradation.

The statistical significance can be evaluated by using the F-value, p-value and adequate precision. From table 2, the F-value of 724.63 implied that the model was significant and there was only 0.01% that the F-value could occur due to noise. Furthermore, the p-value of less than 0.0500 also suggested that the model terms were significant. In this study, the model coefficients of the A, B, C, AB, AC, BC, A^2, B^2, and C^2 were the significant model terms. Among the models, the AB model showed the highest F-value, suggesting that the interactions between light intensity and UV reduction duration were highly significant. The F-value for the lack of fit was 1.42, indicating that the lack of fit was not significant relative to the pure error. Adequate precision is the ratio of signal to noise, in which a ratio of greater than 4 is highly desirable. From the ANOVA results, a ratio of 96.076 was obtained, suggesting that there was an adequate signal and this model could be used.

Figure 6 presents all the diagnostic plots in the evaluation of the adequacy of the model prediction. The normality of the results was checked by plotting the normal probability versus studentized residuals, as shown in figure 6(a). The outcomes of all the experiments were scattered near the diagonal line, implying the good normality of the design. Figure 6(b) revealed the internally studentized residuals versus predicted values. It was reported that the values of the internally studentized residuals have to be within the interval of −3.5 to +3.5 in order to have a good fitting of prediction [22]. As observed in figure 6(b), all the points were observed to be within the range, indicating a good fitting of prediction. The determination of the outlier of the experimental runs was investigated by plotting externally studentized residuals versus the run number. As can be seen in figure 6(c), a good distribution of points was observed with no run out of the desired range, confirming that no outlier was present. The predicted values were compared with the experimental values in order to evaluate the validity of the prediction. As shown in figure 6(d), all the points were scattered very closely to the diagonal line, revealing that the predicted and experimental values were in good agreement.

Figure 7 illustrates the effect of light intensity and UV reduction duration on the photocatalytic performance of the composite photocatalyst with the GO loading of 5 wt%. The selected range of UV light intensity was coded as −1 (0.4 mW cm^{-2}), 0 (8 mW cm^{-2}), and 1 (18 mW cm^{-2}). The region between −1 to 0 was categorized as low UV light intensity, whereas, the region between 0 and 1 was categorized as high UV light intensity. On the other hand, the range of selected UV reduction duration was coded as −1 (6 h), 0 (12 h), and −1 (24 h). It was

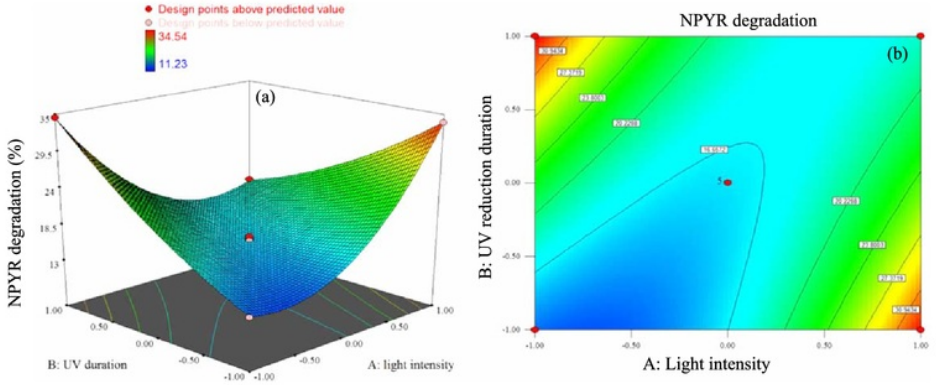

Figure 7. Effect of interaction between the light intensity and the UV reduction time expressed in (a) 3D response surface and (b) contour plot with the GO loading was kept constant at 5 wt%.

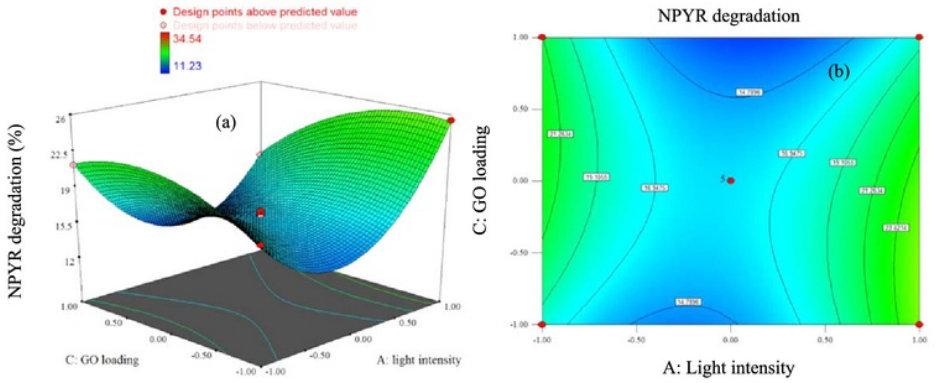

Figure 8. Effect of interaction between the UV light intensity and the GO loading expressed in (a) 3D response surface and (b) contour plot with UV reduction duration kept constant at 12 h.

observed that the rGO-*m*CN prepared under different UV light intensities and UV reduction duration times exhibited different photocatalytic performances. At low UV light intensity, the NPYR degradation increased steadily when the UV reduction duration was prolonged. Conversely, at high UV light intensity, the NPYR degradation decreased gradually with the increasing of UV reduction duration. From figure 7, it was discovered that the optimum UV light intensity and UV reduction duration to prepare the rGO-*m*CN was under UV light intensity of 0.4 mW cm^{-2} for 24 h.

Figure 8 depicts the effects of the light intensity and the GO loading on the photocatalytic performance of the composite when the UV reduction duration was kept constant at 12 h. In low UV light intensity region, the effect of UV light intensity and GO loading was not significant on the NPYR degradation up to a point, in which the NPYR degradation started to increase slightly with the GO loading. In high UV light intensity region, it was obvious that the NPYR degradation decreased gradually with the increase of the GO loading. Optimum UV light intensity and GO loading with UV reduction duration kept constant at 12 h was 18 mW cm^{-2} and 10 wt%, respectively.

Figure 9 presents the effect of the UV reduction duration and the GO loading on the photocatalytic performance of the composite photocatalysts with UV light intensity at 8 mW cm^{-2}. There was no significant change in the NPYR degradation when the composite photocatalyst was prepared at short UV reduction duration and low amount of GO loading. However, at the same UV reduction duration region, the NPYR degradation began to drop significantly when the GO loading amount was high. At the long UV reduction duration region, the NPYR degradation slowly increased with the increasing of GO loading (at low GO loading region) until a point where the NPYR degradation remained almost constant before it started to decrease at high

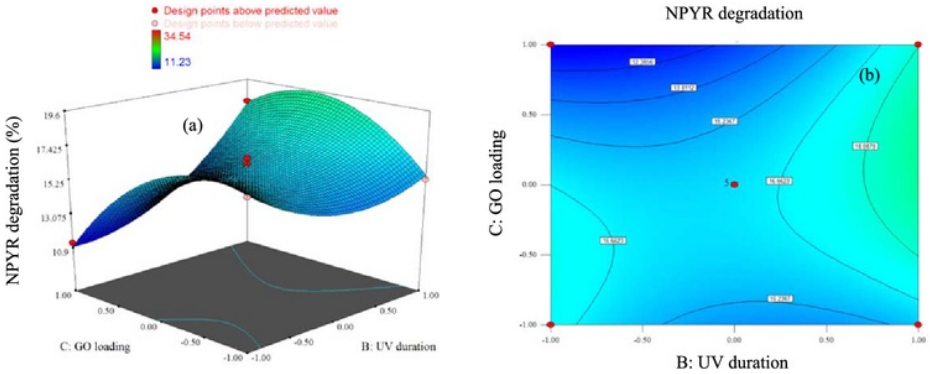

Figure 9. Effect of interaction between the UV duration and the GO loading expressed in (a) 3D response surface and (b) contour plot with UV light intensity kept constant at 8 mW cm^{-2}.

Table 3. Optimum values of the synthesis variables for maximum NPYR degradation by the rGO-*m*CN composite photocatalyst.

Optimum condition			NPYR degradation (%)	
UV light intensity (mW cm^{-2})	UV reduction duration (h)	GO loading (wt%)	Predicted	Experimental
0.40	24.00	5.00	34.51	34.61

GO loading region. Optimum UV reduction duration and GO loading to prepare the composite under UV light intensity of 8 mW cm^{-2} was found to be 24 h and 10 wt%, respectively.

A numerical optimization of the Box-Behnken design in Design-Expert was selected to obtain the maximum vlue of the D. With this approach the optimum synthesis condition (D = 0.999) with the maximized NPYR degradation was conducted with UV light intensity of 0.4 mW cm^{-2} for 24 h at the GO loading of 5 wt%. As illustrated in table 3, the experimental NPYR degradation value (34.61%) was very close to the predicted value (34.51%). This indicated that the predicted model exhibited high accuracy and suitability. Based on the findings, the optimum synthesis conditions to prepare the rGO-*m*CN composite can be proposed as followed. The synthesis process shall be carried out under ambient conditions with the low UV light intensity (0.4 mW cm^{-2}), the long UV reduction duration (24 h), and the moderate amount of GO loading (5 wt%). These parameters suggested that a low UV light intensity is sufficient to reduce the GO to the desired reduction degree with less topological defects at prolonged UV reduction time. In this study, even though the UV reduction duration was shorter, the high UV light intensity was less desired as more topological defects were formed on the GO.

In order to understand the role of the active species for the photodegradation of the NPYR, the effect of two radical scavengers, which were BQ and AO, were investigated on the optimized rGO-*m*CN composite samples. The activity of the rGO-*m*CN composite decreased from 34 to 25% when BQ as the $O_2^{\cdot-}$ radical scavenger was added into the reaction. These findings revealed that $O_2^{\cdot-}$ radicals were important for the degradation of NPYR on the rGO-*m*CN. On the other hand, with the addition of AO as a hole scavenger, the percentage degradation of NPYR on the rGO-*m*CN was more significantly retarded from 34 to 17%. Based on the scavenger studies, it can be concluded that the availability of both holes and $O_2^{\cdot-}$ radicals were crucial in the photodegradation of NPYR on the rGO-*m*CN, where the degradation of NPYR on the rGO-*m*CN was depended more greatly on the photogenerated holes.

The mechanism for the NPYR degradation on the rGO-*m*CN composite photocatalyst could be proposed as followed. Under visible light irradiation the *m*CN would absorb the photon energy and electron-hole pairs would be photogenerated. Some of the photoexcited electrons were transferred from the conduction band of the *m*CN to the rGO due to good electron conductivity of the rGO, which would reduce oxygen to produce the $O_2^{\cdot-}$ radicals. In addition, the unreduced GO itself would produce electron-hole pairs upon irradiation. The photoexcited electrons of the unreduced GO would move to the surface to be used to produce $O_2^{\cdot-}$ radicals. The $O_2^{\cdot-}$ radicals and the photogenerated holes would then degrade the NPYR into oxidized products.

4. Conclusion

The rGO-*m*CN composites prepared by the *in situ* photocatalytic reduction method showed better photocatalytic activity for NPYR degradation than those prepared via thermal annealing, chemical reduction and physical mixing methods. The UV light intensity and UV reduction duration gave significant effects on the photocatalytic performance of the rGO-*m*CN toward NPYR degradation, even though there were no apparent changes in the structural properties. The optimum UV reduction duration in synthesizing the rGO-*m*CN was determined to be 24 h when the UV light intensity was 0.4 mW cm^{-2}. The predicted optimum synthesis condition in the RSM analysis matched well with the experimental synthesis condition. The most significant interaction to be highlighted in the synthesis condition by the photocatalytic reduction method was the effect of UV light intensity and UV reduction duration.

Acknowledgments

Supports from Directorate General of Strengthening Research and Development, Ministry of Research, Technology and Higher Education of the Republic of Indonesia via the Fundamental Research Scheme (PD 2019, No. 058/SP2H/LT/MONO/L7/2019 and No. 001/MACHUNG/LPPM/SP2H-LIT-MONO/III/2019) and the International Research Collaboration and Scientific Publication Grant (PKLN 2018, No. 061/SP2H/LT/K7/KM/2018 and No. 007/MACHUNG/LPPM/SP2H-LIT/II/2018) are greatly acknowledged.

ORCID iDs

Leny Yuliati https://orcid.org/0000-0003-1600-5757
Hendrik O Lintang https://orcid.org/0000-0002-1911-8100

References

[1] Sudha D and Sivakumar P 2015 *Chem. Eng. Proc.: Proc. Intensification* 97, 112
[2] Boyjoo Y, Sun H, Liu J, Pareek V K and Wang S 2017 *Chem. Eng. J.* **310** 537
[3] Ray C and Pal T 2017 *J. Mater. Chem.* A **5** 9465
[4] Zhang N, Zhang Y and Xu Y-J 2012 *Nanoscale* **4** 5792
[5] Tu W, Zhou Y and Zou Z 2013 *Adv. Funct. Mater.* **23** 4996
[6] Xiang Q, Yu J and Jaroniec M 2012 *Chem. Soc. Rev.* **41** 782
[7] An X and Yu J C 2011 *RSC Adv.* **1** 1426
[8] Upadhyay R K, Soin N and Roy S S 2014 *RSC Adv.* **4** 3823
[9] Chua C K and Pumera M 2013 *J. Mater. Chem.* A **1** 1892
[10] Lu G, Ocala L E and Chen J 2009 *Nanotechnology* **20** 445502
[11] Park S and Ruoff R S 2009 *Nat. Nanotechnol.* **4** 217
[12] Kuila T, Mishra A K, Khanra P, Kim N H and Lee J H 2013 *Nanoscale* **5** 52
[13] Dreyer D R, Park S, Bielawski C W and Ruoff R 2010 *Chem. Soc. Rev.* **39** 228
[14] Wong C H, Ambrosi A and Pumera M 2012 *Nanoscale* **4** 4972
[15] Tiong P, Lintang H O, Endud S and Yuliati L 2015 *Adv. Mater. Res.* **1112** 184
[16] Tiong P, Lintang H O, Endud S and Yuliati L 2015 *RSC Adv.* **5** 94029
[17] Hussin F, Lintang H O, Lee S L and Yuliati L 2017 *J. Photochem. Photobiol.* A **340** 128
[18] Williams G, Seger B and Kamat P V 2008 *ACS Nano* **2** 1487
[19] Cao S, Low J, Yu J and Jaroniec M 2015 *Adv. Mater.* **27** 2150
[20] Zhao Z, Sun Y and Dong F 2015 *Nanoscale* **7** 15
[21] Low J, Cao S, Yu J and Wageh S 2014 *Chem. Commun.* **50** 10768
[22] Ba-Abbad M M, Chai P V, Takriff M S, Benamor A and Mohammad A W 2015 *Mater. Des.* **86** 948
[23] Badli N A, Ali R, Bakar W A W A and Yuliati L 2017 *Arab. J. Chem.* **10** 935
[24] Koh P W, Yuliati L and Lee S L 2019 *Iran. J. Sci. Technol. Trans. Sci.* **43** 95
[25] Asghar A, Raman A A A and Daud W M A W 2014 *The Sci. World J.* **2014** 869120
[26] Sivarao S, Milkey K R, Samsudin A R, Dubey A K and Kidd P 2014 *Jordan J. Mech. Indust. Eng.* **8** 35 http://jjmie.hu.edu.jo/Vol8.html
[27] Desai K M, Survase S A, Saudagar P S, Lele S S and Singhal R S 2008 *Biochem Eng. J.* **41** 266
[28] Pilkington J L, Preston C and Gomes R L 2014 *Indust. Crops. Products* **58** 15
[29] Maran J P and Priya B 2015 *Ultrason. Sonochem.* **23** 192
[30] Marcano D C, Kosynkin D V, Berlin J M, Sinitskii A, Sun Z, Slesarev A, Alemany L B, Lu W and Tour J M 2010 *ACS Nano* **4** 4806
[31] Joglekar A M and May A T 1987 *Cereal Food World* **32** 857

MRE2019_3

ORIGINALITY REPORT

23%	6%	21%	7%
SIMILARITY INDEX	INTERNET SOURCES	PUBLICATIONS	STUDENT PAPERS

PRIMARY SOURCES

1	Faisal Hussin, Hendrik O. Lintang, Siew Ling Lee, Leny Yuliati. "Photocatalytic synthesis of reduced graphene oxide-zinc oxide: Effects of light intensity and exposure time", Journal of Photochemistry and Photobiology A: Chemistry, 2017 Publication	4%
2	Hendrik O Lintang, Nurul Husna Sabran, Siew Ling Lee, Leny Yuliati. "Luminescent group 11 3, 5-dimethyl pyrazolate complexes/titanium oxide composites for photocatalytic removal and degradation of 2, 4-dichlorophenoxyacetic acid", Materials Research Express, 2019 Publication	2%
3	Muneer M. Ba-Abbad, Pui Vun Chai, Mohd S. Takriff, Abdelbaki Benamor, Abdul Wahab Mohammad. "Optimization of nickel oxide nanoparticle synthesis through the sol–gel method using Box–Behnken design", Materials & Design, 2015 Publication	2%

4	Tiong, Peggy, Hendrik O. Lintang, Salasiah Endud, and Leny Yuliati. "Improved interfacial charge transfer and visible light activity of reduced graphene oxide–graphitic carbon nitride photocatalysts", RSC Advances, 2015. Publication	1%
5	Leny Yuliati, Shu Chin Lee, Hendrik O. Lintang. "Photocatalytic degradation of aromatic organic pollutants: bulk versus mesoporous carbon nitride", Materials Today: Proceedings, 2019 Publication	1%
6	Nan Zhang, Min-Quan Yang, Siqi Liu, Yugang Sun, Yi-Jun Xu. "Waltzing with the Versatile Platform of Graphene to Synthesize Composite Photocatalysts", Chemical Reviews, 2015 Publication	1%
7	Alim, Nor Shuhada, Hendrik O. Lintang, and Leny Yuliati. "Photocatalytic removal of phenol over titanium dioxide- reduced graphene oxide photocatalyst", IOP Conference Series Materials Science and Engineering, 2016. Publication	1%
8	Leny Yuliati, Nor Shuhada Alim, Hendrik O. Lintang. "Improving the activity of rutile titanium dioxide with reduced graphene oxide", AIP Publishing, 2017 Publication	1%

9	Tan-hua Liu, Xiao-juan Chen, You-zhi Dai, Lu-lu Zhou, Jing Guo, Shuang-shuang Ai. "Synthesis of Ag3PO4 immobilized with sepiolite and its photocatalytic performance for 2,4-dichlorophenol degradation under visible light irradiation", Journal of Alloys and Compounds, 2015 Publication	<1%
10	Shu Chin Lee, Hendrik O Lintang, Leny Yuliati. " High photocatalytic activity of Fe O /TiO nanocomposites prepared by photodeposition for degradation of 2,4-dichlorophenoxyacetic acid ", Beilstein Journal of Nanotechnology, 2017 Publication	<1%
11	Submitted to University of Strathclyde Student Paper	<1%
12	Zhenxun Huang. "Photo-Initiated Dispersion Polymerization of Copolymer Microspheres in a Closed System: Poly(MMA-co-MAA)", Macromolecular Chemistry and Physics, 07/16/2010 Publication	<1%
13	Submitted to Higher Education Commission Pakistan Student Paper	<1%

onlinelibrary.wiley.com

14	Internet Source	<1%
15	Lee, Shu Chin, Hendrik O. Lintang, and Leny Yuliati. "Photocatalytic removal of phenol under visible light irradiation on zinc phthalocyanine/mesoporous carbon nitride nanocomposites", Journal of Experimental Nanoscience, 2014. Publication	<1%
16	conservancy.umn.edu Internet Source	<1%
17	china.iopscience.iop.org Internet Source	<1%
18	Pei Wen Koh, Mohd Hayrie Mohd Hatta, Siew Teng Ong, Leny Yuliati, Siew Ling Lee. "Photocatalytic degradation of photosensitizing and non-photosensitizing dyes over chromium doped titania photocatalysts under visible light", Journal of Photochemistry and Photobiology A: Chemistry, 2017 Publication	<1%
19	Yee Khai Ooi, Faisal Hussin, Leny Yuliati, Siew Ling Lee. "Comparison study on molybdena-titania supported on TUD-1 and TUD-C synthesized via sol-gel templating method: Properties and catalytic performance in olefins	<1%

epoxidation", Materials Research Express, 2019
Publication

20	www.researchgate.net Internet Source	<1%
21	Nikzad, Maryam, Kamyar Movagharnejad, Farid Talebnia, Ziba Aghaiy, and Moein Mighani. "Modeling of Alkali Pretreatment of Rice Husk Using Response Surface Methodology and Artificial Neural Network", Chemical Engineering Communications, 2014. Publication	<1%
22	L Yuliati, A M Salleh, M H M Hatta, H O Lintang. "Effect of preparation methods on the activity of titanium dioxide-carbon nitride composites for photocatalytic degradation of salicylic acid", IOP Conference Series: Materials Science and Engineering, 2018 Publication	<1%
23	Submitted to National Yunlin University of Science and Technology Student Paper	<1%
24	Submitted to University of Nottingham Student Paper	<1%
25	www.frontiersin.org Internet Source	<1%

26	SAWINDER KAUR. "RESPONSE SURFACE OPTIMIZATION OF CONDITIONS FOR THE CLARIFICATION OF GUAVA FRUIT JUICE USING COMMERCIAL ENZYME", Journal of Food Process Engineering, 08/2009 Publication	<1%
27	Muhammad Mubaraki. "Comparison of laboratory performance of two superpave binders mixed with two modifiers", Road Materials and Pavement Design, 2018 Publication	<1%
28	Nguyen, Bich Ha, Van Hieu Nguyen, and Dinh Lam Vu. "Photocatalytic composites based on titania nanoparticles and carbon nanomaterials", Advances in Natural Sciences Nanoscience and Nanotechnology, 2015. Publication	<1%
29	Muhammad R Islam. "Schottky diode via dielectrophoretic assembly of reduced graphene oxide sheets between dissimilar metal contacts", New Journal of Physics, 03/23/2011 Publication	<1%
30	Jain, S.. "Use of malachite green as photocatalyst in reduction of sodium and potassium carbonates", Energy Conversion and Management, 200405	<1%

Publication

31	tel.archives-ouvertes.fr Internet Source	<1%
32	Jian Gao, Zhichun Si, Yunfan Xu, Liping Liu, Yuanyuan Zhang, Xiaodong Wu, Rui Ran, Duan Weng. " Pd–Ag@CeO Catalyst of Core–Shell Structure for Low Temperature Oxidation of Toluene Under Visible Light Irradiation ", The Journal of Physical Chemistry C, 2018 Publication	<1%
33	L Yuliati, S Z M So'ad, N S Alim, H O Lintang. "Fluorescence Sensing of Nitrite Ions on Polyvinylpyrrolidone/Zinc Oxide Composites Prepared by Impregnation Method", IOP Conference Series: Materials Science and Engineering, 2017 Publication	<1%
34	Submitted to Nanyang Technological University, Singapore Student Paper	<1%
35	Submitted to Universidade do Porto Student Paper	<1%
36	Zhengdong Zhang. "Photografting of unable-to-be-irradiated surfaces. I. Batch vapor-phase process by one-step method", Journal of Applied Polymer Science, 08/15/2006 Publication	<1%

37	Modirshahla, N.. "Decolorization and mineralization of C.I. Acid Yellow 23 by Fenton and photo-Fenton processes", Dyes and Pigments, 2007 Publication	<1%
38	Rosset, Michele, Vinicius Ricardo Acquaro, and Adelaide Del Pino BelÃ©ia. "Protein Extraction from Defatted Soybean Flour with Viscozyme L Pretreatment : Protein Extraction from Defatted Soy Flour", Journal of Food Processing and Preservation, 2012. Publication	<1%
39	Submitted to Monash University Sunway Campus Malaysia Sdn Bhd Student Paper	<1%
40	Submitted to Punjab Technical University Student Paper	<1%
41	Shen, Y.S.. "Decomposition of gas-phase chloroethenes by UV/O"3 process", Water Research, 199809 Publication	<1%
42	Submitted to Plano Independent School District Student Paper	<1%
43	Siah, Wai Ruu, Hendrik O Lintang, Mustaffa Shamsuddin, and Leny Yuliati. "High photocatalytic activity of mixed anatase-rutile	<1%

phases on commercial TiO2 nanoparticles", IOP Conference Series Materials Science and Engineering, 2016.
Publication

---

44 Submitted to Technical University of Cluj-Napoca
Student Paper
<1%

---

45 landreclamationjournal.usamv.ro
Internet Source
<1%

---

46 Submitted to Indian Institute of Science Education and Research
Student Paper
<1%

---

47 Tang, Ing Hua, Rita Sundari, Hendrik O Lintang, and Leny Yuliati. "Detection of nitrite and nitrate ions in water by graphene oxide as a potential fluorescence sensor", IOP Conference Series Materials Science and Engineering, 2016.
Publication
<1%

---

48 sevgiligiyim.com
Internet Source
<1%

---

49 Lee, Shu Chin, Norhasnita Hasan, Hendrik O. Lintang, Mustaffa Shamsuddin, and Leny Yuliati. "Photocatalytic removal of 2,4-dichlorophenoxyacetic acid herbicide on copper oxide/titanium dioxide prepared by co-precipitation method", IOP Conference Series
<1%

Materials Science and Engineering, 2016.
Publication

50	R. Ramasamy, V. Selvarajan, K. Ramachandran. "Characterization of DC plasma spray torch using energy balance technique and thermo-fluid dynamical consideration", Plasma Devices and Operations, 1997 Publication	<1%
51	Submitted to Universiti Teknologi MARA Student Paper	<1%
52	Jinlong Zhang, Baozhu Tian, Lingzhi Wang, Mingyang Xing, Juying Lei. "Photocatalysis", Springer Science and Business Media LLC, 2018 Publication	<1%

Exclude quotes	Off	Exclude matches	Off
Exclude bibliography	On		